EurJIC
European Journal of Inorganic Chemistry

A Journal of ChemPubSoc Europe

**Title:** Synthesis of hierarchical SAPO-5 & SAPO-34 materials via post-synthetic alkali treatment and their enhanced catalytic activity in transesterification reaction

**Authors:** Divya Jadav, Rajib Bandyopadhyay, and Mahuya Bandyopadhyay

**To be cited as:** *Eur. J. Inorg. Chem.* 10.1002/ejic.201901250

**Link to VoR:** http://dx.doi.org/10.1002/ejic.201901250

WILEY-VCH

10.1002/ejic.201901250

# Synthesis of hierarchical SAPO-5 & SAPO-34 materials via post-synthetic alkali treatment and their enhanced catalytic activity in transesterification reaction

Divya Jadav[a] Rajib Bandyopadhyay,[b] and Mahuya Bandyopadhyay*[a]

**Abstract:** SAPO-5 and SAPO-34 materials were modified using post-synthetic alkali treatment which results in the formation of hierarchical SAPO-5 and SAPO-34 materials. To evident the generation of mesoporosity, modified materials were thoroughly characterized using XRD, FE-SEM, TGA, ICP-OES and $N_2$ adsorption/desorption techniques. Alkali treated SAPO-5 and SAPO-34 materials were utilized for transesterification of triacetin model reaction, at optimized conditions by varying catalyst amount and reaction time. 90% triacetin conversion with 66% methyl acetate yield was achieved using modified SAPO-5 catalyst whereas, 68% triacetin conversion with 37% methyl acetate yield was achieved using modified SAPO-34 catalyst and the alkali treated SAPO-5 catalyst was stable upto 4th cycle.

## Introduction

Crystalline aluminophosphate (AlPO-n) and silicoaluminophosphate (SAPO-n) molecular seives are of great interest for their hydrothermal stability and potential application in adsorption, catalysis and ion-exchange processes.[1,2] A large number of work has been reported on the synthesis and modification of different SAPO materials to modify and improve their physico-chemical properties and extensively studied in several catalytic applications.[3-6] Hierarchical zeolites were prepared through post-synthetic process by removing framework atoms using demetallation method. [7] Many reports are available based on the modification of different zeolites using various alkaline treatments and their subsequent catalytic applications. Alkali treatment on these material leads to generation of mesoporosity by means of desilication in the framework structure [8-10], whereas acid treatment leads to dealumination for the formation of mesopore in the framework.[11-14] The intrinsic properties of materials can be tailored by surface modification; for example, the acidity of BEA zeolite can be controlled using alkali ion-exchange treatment, and after modification it showed improved catalytic activity in the production of isobutylene from acetone.[15] Moreover, hierarchical SAPO-5, SAPO-34, ZSM-5, ZSM-48, MCM-22, Zn-SAPO-34, and H-β zeolite type of materials were prepared using different alkali treatment through post-synthesis route and their catalytic performance was found to be better than that of as made zeolites.[16-26] Verboekend et al. reported synthesis of hierarchical silicoaluminophosphate by using different acid and base treatments and their catalytic application in model alkylation reaction of benzyl alcohol with toluene.[27] Surface basicity was generated on MCM-22 and H-Y zeolite using NaOH solution with different concentrations and the modified zeolites were used in transesterification of triolein, which showed conversion up to 98%. It was observed that the crystallinity of modified material decreased after alkali treatment. However, modified materials were more effective in transesterification reaction.[28] There are also other reports available on NaOH ion-exchanged zeolite beta and MCM-22, which were found to be catalytically active in transesterification of triglycerides with 95% conversion.[29]

Nowadays, researchers are taking immense interest in minimizing heavy consumption of fossil fuels by inventing feasible routes for biodiesel production. Biodiesel is found to be a promising alternative of fossil fuels as they can reduce the greenhouse effect by their use as a transport fuel.[30,31] It can be produced by either transesterification or esterification of free fatty acids using homogeneous as well as heterogeneous catalysts. Heterogeneous catalysis manifests a powerful strategy to overcome the conventional drawbacks of homogeneous catalysis such as emulsification, product separation and impure products by easy separation and reusability. A lot of work has been reported using heterogeneous catalysis for biodiesel production.[30,32,33] Both acid or base can catalyze the transesterification reaction. Some studies are focused on the development of environmentally benign heterogeneous base-catalyzed transesterification reactions.[33,34] Du et al. reported preparation of NaY supported $La_2O_3$ catalysts and its application in transesterification of castor oil to biodiesel.[35] In some of our previous studies, acid-base functionalized mesoporous MCM-48, SBA-15 and MCM-41 were

---

[a] Institute of Infrastructure, Technology, Research and Management, IITRAM, Maninagar, Ahmedabad, Gujarat, India; https://iitram.ac.in/Faculty
E-mail address: mahuyabandyopadhyay@iitram.ac.in
[b] School of Technology, Pandit Deendayal Petroleum University, Raisan, Gandhinagar, Gujarat, India; http://sot.pdpu.ac.in/sot-faculty.html

prepared using APTES (aminopropyl triethoxysilane) and MPTES (mercaptopropyl triethoxysilane) through post-synthetic modification and were found to play significant role in transesterification of triacetin.[36,37]

Inspired by the applications of alkali treated materials in various important chemical reactions, our aim in this work was to modify SAPO-5 and SAPO-34 materials using post-synthetic alkali treatment. To our knowledge there is no report so far on alkali treated SAPO-5 and SAPO-34 materials for the application in transesterification reaction. Thorough characterization of the materials was performed to explore the hierarchical structure-property relationship using different physicochemical techniques. Alkali treated SAPO-5 and SAPO-34 catalysts were tested in transesterification of triacetin reaction under various conditions to achieve optimal triacetin conversion and methyl acetate yield.

## Results and Discussion

### Catalyst Characterization

XRD measurement was performed to identify the phase purity and crystallinity of the SAPO-5 and SAPO-34 materials. Figure 1 shows the XRD patterns of as made and modified materials. XRD patterns of as made SAPO-5 material reveals pure SAPO-5 phase and homogeneity was maintained even after the treatment with decrease in peak intensity. It was observed that 5 h and 8 h treated SAPO-5 has almost similar crystallinity but some peaks after 25° 2θ were missing in 8 h treated SAPO-5 material. Highly crystalline SAPO-34 material was obtained but the crystallinity of the samples was deteriorated after alkali treatment and only two significant peaks were observed for SAPO-34-5h-AT. However, SAPO-34-8h-AT material showed no crystallinity, indicative of structural deterioration or collapsing with prolonged alkali treatment, which in good agreement with the literature report. [27]

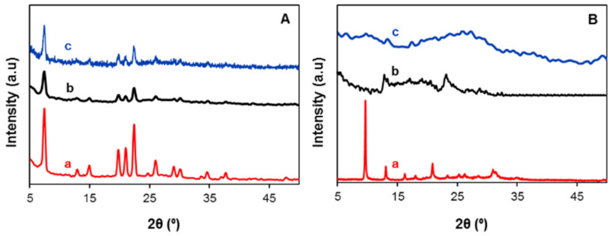

**Figure 1.** Powder XRD patterns of (a) as made, (b) 5 h alkali treated and (c) 8 h alkali treated (A) SAPO-5 and (B) SAPO-34 materials.

As shown in Figure 2, low angle XRD in the range of 1.5° to 10° 2θ was performed for SAPO-5-5h-AT and SAPO-34-5h-AT materials. An intense peak was observed at 1.58° 2θ for SAPO-5-5h-AT, which is typical for mesoporous phase and another prominent peak at 7.5° 2θ with a small fringe at 7.7° 2θ was identified in SAPO-5-5h-AT, which is a confirmation of formation of lamellar type of mesoporous phase.[17,18] However, SAPO-5 also shows its first microporous peak at 7.5° 2θ. Both the peaks have overlapped due to almost same 2θ value. In case of SAPO-34 two peaks at 1.77° and 7.49° 2θ values were observed. The peak at 1.77° 2θ is typical for hierarchical mesoporous structure indicative of generation of mesoporosity in SAPO-34 material. The presence of two intense peaks at 1.77° and 7.49° 2θ value is a sign of formation of pure lamellar phase in SAPO-34-5h-AT material.[18] These facts imply that, the SAPO-5 material was successfully modified and generation of additional porosity was not detrimental to the SAPO-5 (AFI) phase; whereas in SAPO-34-5h-AT, only mesoporous peak was observed after treatment. The fact suggests that different crystal structures behave differently with same treatment and the small pore size of SAPO-34 could not fully withstand the effect of modification.

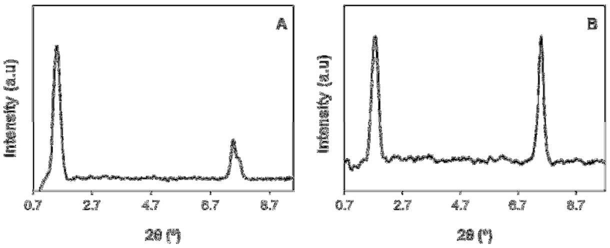

**Figure 2.** Low angle XRD patterns of (A) SAPO-5-5h-AT and (B) SAPO-34-5h-AT materials.

SEM images of pure and modified SAPO-5 and SAPO-34 materials are depicted in Figure 3. It shows the morphology change in both the materials after modification. SEM image of as made SAPO-5 revealed hexagonal sheet-like plates with 2 µm length and 1 µm breadth. Combined hexagonal particles of SAPO-5 show spherical morphology (Fig. 3 A(b) and crystals of SAPO-5 material agglomerated after modification with decrease in the crystal size, may be due to the formation of mesoporosity inside the microporous SAPO-5 material. Cubic morphology of as made SAPO-34 with 1 µm length and breadth was confirmed. After modification, the shape and size of the SAPO-34 did not show any significant changes.

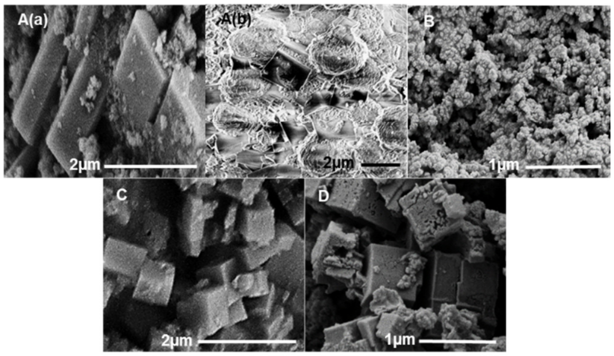

**Figure 3.** SEM images of [A](a) as made SAPO-5 in hexagonal particles, [A](b) as made SAPO-5 in spherical morphology, [B] SAPO-5-5h-AT, [C] as made SAPO-34 and [D] SAPO-34-5h-AT.

$N_2$ adsorption/desorption studies of alkali treated SAPO-5 and SAPO-34 show both Type-I and Type-IV isotherms as shown in Figure 4 A. Both isotherm shows characteristic hysteresis loop between the partial pressure ($p/p_o$) 0.4-1 is an evidence for the formation of mesoporosity after base treatment.

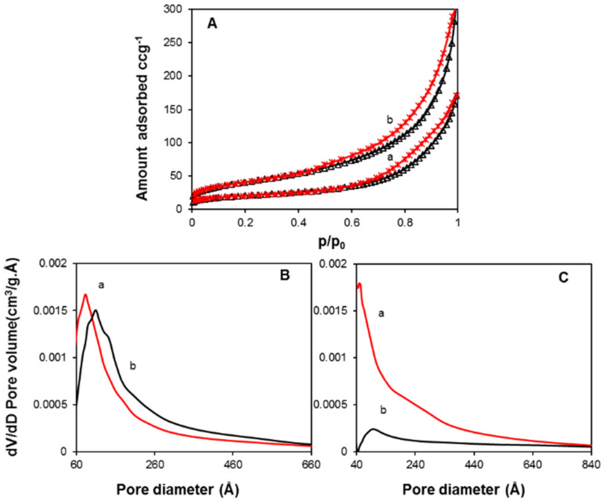

**Figure 4.** (A) $N_2$ adsorption/desorption isotherm of (a) SAPO-5-5h-AT and (b) SAPO-34-5h-AT. (B) Pore size distribution of (a) as made SAPO-5 and (b) SAPO-5-5h-AT. (C) Pore size distribution of (a) as made SAPO-34 and (b) SAPO-34-5h-AT.

Textural properties of the as made and alkali treated materials are depicted in Table 1. The pore volume and pore diameter considerably increased after modification due to generation of mesoporosity, which resembles with the fact already reported elsewhere.[16,18] The pore volume of as made SAPO-5 was 0.102 $cm^3/g$ and it has increased after modification to 0.266 $cm^3/g$ for SAPO-5-5h-AT. Total pore volume for as made SAPO-34 was 0.117 $cm^3/g$ and 0.469 $cm^3/g$ after modification (SAPO-34-5h-AT).

**Table 1.** Textural properties of as made and modified SAPO-5 and SAPO-34 materials

| **Catalyst** | **Pore volume ($cm^3/g$) [a]** | | | **Pore diameter (Å) [a]** | **Si (%) [b]** | **Si/Al ratio [b]** |
|---|---|---|---|---|---|---|
| | **Total** | **Micro** | **Meso** | | | |
| SAPO-5 | 0.102 | - | - | 109 | 0.066 | 0.110 |
| SAPO-5-5h-AT | 0.266 | 0.004 | 0.262 | 128 | 0.034 | 0.054 |
| SAPO-34 | 0.117 | - | - | 97 | 0.111 | 0.200 |
| SAPO-34-5h-AT | 0.469 | 0.002 | 0.467 | 109 | 0.091 | 0.147 |

[a] determined from BJH method. [b] determined by ICP-OES analysis.

As shown in Figure 4 B and C, pore diameter also increased after modification. The pore size increased from 109 Å to 128 Å after alkali treatment in SAPO-5 material whereas in SAPO-34 it increased from 97 Å to 109 Å. Apart from $N_2$ adsorption, low angle XRD and SEM analyses, the generation of mesoporosity is also directly supported by ICP-OES results. Si/Al ratio decreases after alkali treatment (Table 1) due to desilication in SAPO-5 and SAPO-34 material resulting in additional porosity.[19]

Thermogravimetric analysis (TGA) of alkali treated SAPO-5 and SAPO-34 materials (Fig. 5) exhibits total three stage weight loss. First weight loss below 200 ℃ is due to the loss of physisorbed water molecules. Second weight loss in the temperature range of 200-400 ℃ is due to decomposition of some part of TEA (SDA) in SAPO-5 and TEAOH (SDA) SAPO-34. The final weight loss after 400 ℃ is due to decomposition of SDA and TPAOH.[17]

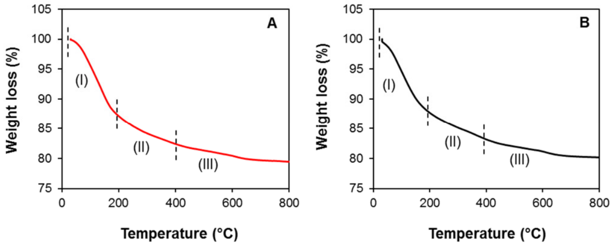

**Figure 5.** Thermogravimetric analysis of (A) SAPO-5-5h-AT and (B) SAPO-34-5h-AT materials.

## Catalytic activity test

### Comparison of various catalysts

Prepared catalysts were evaluated in the transesterification of triacetin with methanol. The dimension of triacetin molecule is around 10.206 × 3.85 Å [38] and pore diameter of SAPO-5-5h-AT and SAPO-34-5h-AT is 128 Å and 109 Å, respectively. Therefore, diffusional limitation of triacetin inside the pore of modified materials can be ignored. Figure 6 shows the triacetin conversion and methyl acetate yield using different catalysts. As the transesterification reaction is an equilibrium-controlled reaction, higher methanol/triacetin ratio was used to shift the equilibrium towards right to get better conversion and more yield.[37]

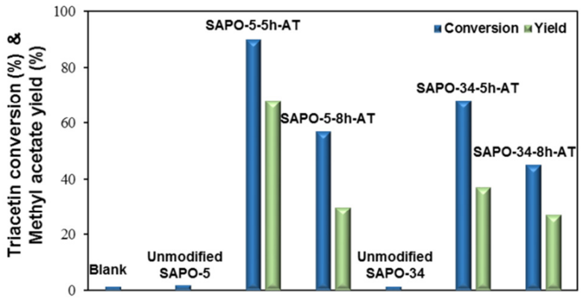

**Figure 6.** Triacetin conversion and methyl acetate yield of as made SAPO-5, SAPO-5-5h-AT, SAPO-5-8h-AT, as made SAPO-34, SAPO-34-5h-AT, SAPO-34-8h-AT and blank.

90% triacetin conversion with 68% methyl acetate yield was achieved using SAPO-5-5h-AT material and 57% conversion with 30% methyl acetate yield was obtained with SAPO-5-8h-AT. SAPO-34-5h-AT gives 68% conversion with 37% methyl acetate yield whereas, SAPO-34-8h-AT shows 45% conversion and 27% yield. The significance of our study in transesterification reaction using alkali treated SAPO-5 and SAPO-34 materials were justified by comparing the triacetin conversion of modified materials with that of blank reaction (without catalyst) and reaction using as made SAPO-5 and SAPO-34 materials. As made SAPO-5 gives 2% conversion, whereas blank and as made SAPO-34 gives negligible conversion (1%). Moreover, prepared catalysts showed higher conversion and yield compared to organic-inorganic hybrid iron(III) phosphonate catalysts and propylsulfonic acid supported aerogel catalysts reported elsewhere [39, 40]. Catalytic results clearly indicate the prominent application of prepared materials in transesterification of triacetin reaction.

## Effect of catalyst amount

The reaction was optimized using different catalyst amount to achieve the best triacetin conversion and the results are depicted in Figure 7. The catalyst amount was varied from 0.1 g to 0.5 g and reaction was performed at 68 °C for 6 h. 0.2 g of SAPO5-5h-AT shows 44% conversion whereas SAPO-5-8h-AT, SAPO-34-5h-AT and SAPO-34-8h-AT shows 11%, 21% and 7% triacetin conversion, respectively. The highest 90% triacetin conversion was achieved using 0.5 g of SAPO-5-5h-AT catalyst. Results indicate that triacetin conversion increases for all the catalysts with increase in the catalyst amount.

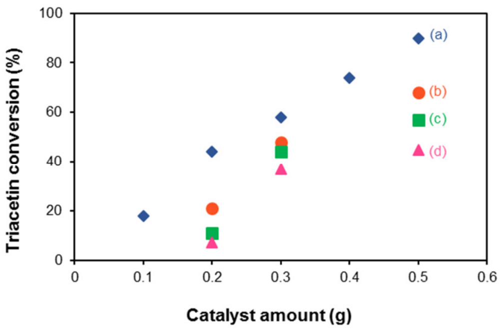

**Figure 7.** Triacetin conversion using different catalyst amount of (a) SAPO-5-5h-AT, (b) SAPO-34-5h-AT, (c) SAPO-5-8h-AT, and (d) SAPO-34-8h-AT.

The reaction was carried out at 72 °C also; however, there was almost no change in conversion and yield (92% conversion and 68% yield for SAPO-5h-AT), so all the reactions were performed at 68 °C, which is close to the boiling point of methanol. The reaction conditions were optimized to get maximum conversion and yield at mild conditions by using minimum amount of catalyst.

The turnover frequency (TOF) was also calculated (Table 2) to compare the availability of active sites and efficiency of catalyst based on the estimated basicity. Basicity of as made SAPO-5 from titration method was found to be 0.56 mmol/g, and 0.79 mmol/g for as made SAPO-34. Alkali treatment leads to increase in the surface basicity of SAPO-5 and SAPO-34 materials. It has been found that the basicity of modified SAPO-5 is lower than that of SAPO-34. However, from the result it is clear that catalytic activity does not solely depend upon basicity. Structure of the catalyst plays an important role towards its activity. TOF values were found to be constant for SAPO-5-5h-AT irrespective of catalyst amount and SAPO-34-5h-AT also showed nearly unchanged TOF values. However, SAPO-5-8h-AT and SAPO-34-8h-AT showed slight variation in TOF values with different catalyst amount.

**Table 2.** TOF, basicity and triacetin conversion with different catalyst amount

| Catalyst | Catalyst amount (g) | Triacetin conversion (%) | Basicity (mmol/g)[a] | TOF (min $^{-1}$) |
|---|---|---|---|---|
| SAPO-5-5h-AT | 0.2 | 44 | 1.07 | 268 |
| | 0.3 | 58 | | 240 |
| | 0.5 | 90 | | 220 |
| SAPO-5-8h-AT | 0.2 | 11 | 1.13 | 80 |
| | 0.3 | 44 | | 160 |
| | 0.5 | 57 | | 131 |
| SAPO-34-5h-AT | 0.2 | 21 | 1.28 | 110 |
| | 0.3 | 48 | | 162 |
| | 0.5 | 68 | | 138 |
| SAPO-34-8h-AT | 0.2 | 7 | 1.32 | 36 |
| | 0.3 | 37 | | 123 |
| | 0.5 | 45 | | 90 |

[a] calculated from titration method using oxalic acid and NaOH.

### Effect of reaction time

For further optimization, transesterification reaction was also performed for different reaction times and the results are shown in Figure 8. SAPO-5-5h-AT showed 28% triacetin conversion after 2 h of reaction time, whereas SAPO-5-8h-AT, SAPO-34-5h-AT and SAO-34-B showed 14%, 16% and 10% conversion, respectively. Maximum 90% conversion was achieved after 6 h of reaction time using SAPO-5-5h-AT catalyst whereas SAPO-5-8h-AT, SAPO-34-5h-AT and SAPO-34-8h-AT gave 57%, 68% and 39% conversion, respectively. As expected, conversion increases with increase in reaction time.

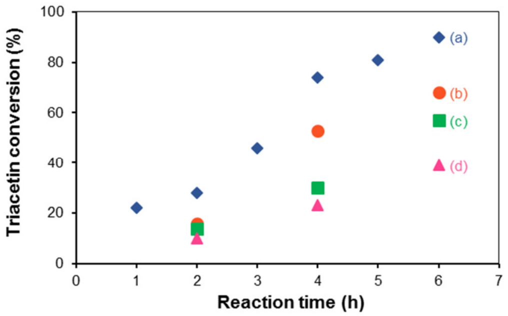

**Figure 8.** Triacetin conversion using (a) SAPO-5-5h-AT, (b) SAPO-34-5h-AT, (c) SAPO-5-8h-AT, and (d) SAPO-34-8h-AT for different reaction time.

Kinetic plot of $\log C_0/C$ vs. time for SAPO-5-5h-AT is given in Figure 9, ($\log C_0/C$ is the value of consumed triacetin, $C_0$ is the initial concentration of triacetin and C is the concentration of triacetin at different time) which shows linear relationship between consumed triacetin and reaction time. This plot indicates that there is no structural degradation in active sites of the SAPO-5-5h-AT catalyst.

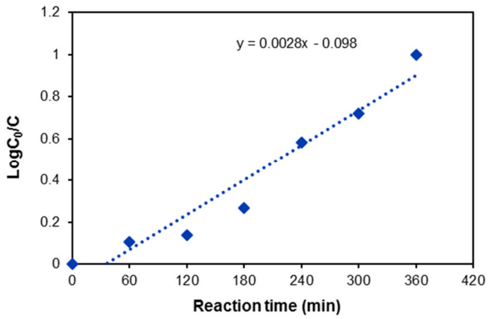

**Figure 9.** Kinetic plot of transesterification of triacetin over SAPO-5-5h-AT catalyst.

### Recyclability of the catalyst

Recyclability is one of the important parameters to serve as robust heterogeneous catalyst. Recyclability test for SAPO-5-5h-AT was performed and the result is summarized in Figure 10. After completion of the reaction, the catalyst was filtered, washed with methanol, dried at room temperature and used for another cycle.

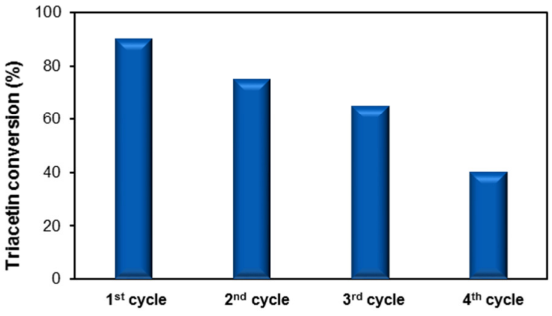

**Figure 10.** Recyclability of SAPO-5-5h-AT catalyst in transesterification of triacetin reaction.

During 1st cycle, it shows 90% conversion and decreases to 75% in the 2nd run. 65% conversion was found in the 3rd cycle and at last 40% conversion was found in the 4th run. Thus SAPO-5-5h-AT was found effective till the 3rd cycle and in the 4th cycle triacetin conversion decreases up to 40% which may be due to

10.1002/ejic.201901250

the deposition of product somewhere in the pores of the catalyst or due to coke formation. However, the triacetin conversion in 4th run is reasonable compared to blank and normal SAPO-5 (1%, Fig. 6). XRD pattern of spent catalyst shows no structural degradation of the SAPO-5 phase (Fig. 11). Comparing all the results it is clear that 5 hour treated SAPO-5-5h-AT catalyst is quite active and stable catalyst for this model transesterification of triacetin reaction.

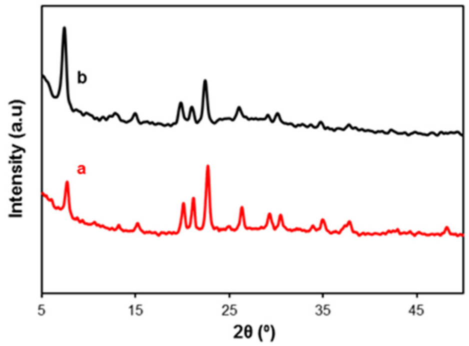

**Figure 11.** Powder XRD patterns of (a) Before reaction SAPO-5-5h-AT & (b) Spent SAPO-5-5h-AT.

## Conclusion

Alkali treatment on SAPO material leads to the formation of mesoporosity with enhanced catalytic activity in transesterification of triacetin reaction. Generation of mesoporosity was evident through powder XRD, SEM, $N_2$ adsorption/desorption isotherm and ICP-OES analyses. Prepared catalysts were tested in transesterification of triacetin reaction and reaction conditions were optimized. Amongst all the modified catalysts, SAPO-5-5h-AT was found prominent as well as an environmentally benign catalyst with 90% triacetin conversion and 68% methyl acetate yield which was also effective till the 4th cycle. From the study of post-synthetic alkali treatment of these catalysts, with combination of all the experimental outcome, it is clear that surface modification leads to improve the structure activity relationship and can be further explored using other acid and base treatment for transesterification of various feedstock.

## Experimental Section

### Synthesis of SAPO-5

Microporous SAPO-5 material was synthesized using hydrothermal synthesis method following literature procedure [41] using molar gel composition of $1.0Al_2O_3$: $1.0P_2O_5$: $0.3SiO_2$: 1.0TEA(SDA): $40H_2O$. In a typical hydrothermal synthesis, calculated amount of aluminium isopropoxide (SDFCL, 97%) and deionized water were mixed in a plastic beaker and stirred at room temperature to form a homogeneous mixture. Dilute o-phosphoric acid (Merck, 85%) was added drop-wise in the mixture with continuous stirring for 20 minutes. Colloidal silica (Sigma Aldrich , Ludox As-40, 40%) was then added slowly in the mixture and allowed to stir for 20 minutes. Subsequently, the template TEA (Triethyl amine, Merck, 99.5%) was added dropwise and whole mixture was stirred for further one and half hour. The complete homogeneous gel was formed and it was transferred in a Teflon lined stainless steel autoclave and subjected to crystallization at 175 °C for 24 hours. After completion of crystallization, the autoclave was cooled to room temperature and the precursor was filtered and washed with deionized water. Finally, microporous SAPO-5 material was dried and collected for further modification.

### Synthesis of SAPO-34

Microporous SAPO-34 material was also synthesized using synthesis procedure from literature[41] with molar gel composition of $1.0Al_2O_3$: $1.0P_2O_5$: $0.6SiO_2$: 1.0TEAOH(SDA): $40H_2O$. The template TEAOH (Tetraethyl ammonium hydroxide, Sigma Aldrich, 40%) was used for SAPO-34 synthesis. The remaining synthesis procedure, crystallization time and crystallization temperature was same as SAPO-5 synthesis.

### Alkali Treatment

As made SAPO-5 and SAPO-34 materials were modified using a mixture of NaOH (Finar, 97%) and TPAOH (Tetra propyl ammonium hydroxide, Sigma Aldrich) solution through post-synthetic method.[42] In a typical procedure, solid as made material was stirred with a mixture of 0.1M NaOH and 1.0M TPAOH solution. The solid-to-liquid ratio was 40 g $L^{-1}$ for NaOH and 200 g $L^{-1}$ for TPAOH. The whole mixture was magnetically stirred in a polypropylene bottle at 70 °C for 5 hours in an oil bath. Subsequently, the solid was filtered using deionized water and dried at room temperature. For comparison, the same treatment was performed for 8 h also. 5 h treated samples were denoted as SAPO-5-5h-AT and SAPO-34-5h-AT whereas 8 h treated samples were denoted as SAPO-5-8h-AT and SAPO-34-8h-AT.

### Basicity Measurement

Total basicity of the modified materials was elucidated by acid-base titration using 0.01M oxalic acid (Merck, 99%) and 0.01M NaOH solutions.[43] Typically, 0.1 g of modified materials were dispersed in 20 ml of 0.01M oxalic acid solution with continuous stirring for 12 h at room temperature (so that, base from the modified material can be consumed by oxalic acid solution). After that, the material was filtered and titrated against 0.01M NaOH solution using phenolphthalein indicator. For the basicity calculation of modified SAPO-5 and SAPO-34 molecular sieves, an oxalic acid solution without catalyst was also titrated against NaOH.

### Characterization

Crystallinity and phase purity of the materials were determined by powder X-ray diffraction (XRD) patterns using PANalytical X'Pert pro equipment with Cu-Kα radiation at 40kV/40 mA. XRD patterns were recorded in the 2θ range of 2-50° with a goniometer speed and step size of 1° per minute and 0.02°, respectively for micro phase identification. Low angle XRD was performed using DY 1251, PANalytical Empyrean Powder X-Ray diffractometer for mesoporous phase identification in modified catalysts with 2θ range of 1.5-10° using 1° per minute rate and 0.01° step size. Surface morphology of the materials was evaluated by scanning electron microscope (SEM) images over Field emission electron microscope (FE-SEM) using Zeiss Ultra 55 instrument. Inductively coupled plasma optical emission spectroscopy (ICP-OES) was performed (Thermo iCAP 7000) to analyze the concentration of Si and Al. $N_2$ adsorption/desorption isotherm was carried out to analyze the textural properties of materials over Micromeritics 3 Flex 3500 analyzer. Prior to the analysis, samples were degassed at 150 ℃ in nitrogen flow for 5 h. The analysis was carried out at liquid nitrogen temperature (77 K) with low pressure. Textural properties such as pore volume and pore diameter of the materials before and after modification were calculated from the analysis. Thermogravimetric (TG) analysis was performed to examine the thermal stability of prepared materials. For TG analysis, Perkin-Elmer (TGA 4000) system was used in air flow (19.8 ml min$^{-1}$) with heating rate of 10 ℃ in the temperature range of 30-800 ℃.

### Catalytic activity measurement

All the modified catalysts were tested in transesterification of triacetin reaction with excess of methanol. Prior to the reaction, Alkali treated SAPO-5 and SAPO-34 materials were activated at 75 ℃ for 1 h. For this model reaction, triacetin (Finar, 99%) and excess methanol (Rankem, 99.8%) (triacetin: methanol molar ratio of 16:1) was taken in a glass culture tube fitted with a screwed cap and stirred to attain the reaction temperature. After that, 0.5 g of the catalyst was added and the reaction was continued for 6 h at

℃. After completion of the reaction, the product was separated from the catalyst by filtration and the catalyst was washed 2-3 times with methanol and dried at room temperature. For each product, Triacetin conversion and methyl acetate yield were analyzed by gas chromatography equipped with flame ionization detector (GC-FID) over Shimadzu GC-2025 fitted with HP-5 column.

## Acknowledgements

We express our sincere thanks to SRDC-PDPU, Gandhinagar for their great support on powder XRD and FE-SEM measurements. We also thank Scientist Dr. Uma Chatterjee at CSMCRI-Bhavnagar for providing BET and low angle XRD analysis. Furthermore, we are thankful to Dr. Prasenjit Mal at NISER-Bhubaneswar for providing FE-SEM measurements. We acknowledge Mr. Rakesh Jha (Thermofisher lab asst.) for ICP analysis and also thankful to Mr. Rakesh Behera at IIT Gandhinagar for TG analysis. Special thanks to Mr. Maaz Nawab and Ms Riddhi Thakkar of PDPU for their help in GC analysis. One of the author (DJ) is thankful to IITRAM-Ahmedabad for a research fellowship.

**Keywords:** Mesoporous SAPO-5 • Mesoporous SAPO-34 • Alkali treatment • Transesterification of triacetin

[1] R. B. Borade, A. Clearfield, *J. Mol. Catal.* **1994**, *88*, 249-266.

[2] J. Chen, P. A. Wright, S. Natarajan, J. M. Thomas, *Stud. Surf. Sci. Catal.* **1994**, *84*, 1731-1738.

[3] S. T. Wilson, *Stud. Surf. Sci. Catal.* **1991**, *58*, 137-151.

[4] S. T. Wilson, *Stud. Surf. Sci. Catal.* **2007**, *168*, 105-135.

[5] P. P. Man, M. Briend, M. J. Peltre, A. Lamy, P. Beaunier, D. Barthomeuf, *Zeolites* **1991**, *11*, 563-572.

[6] D. Young, M. E. Davis, *Zeolites* **1991**, *11*, 277-281.

[7] A. Feliczak-Guzik, *Microporous Mesoporous Mater.* **2018**, *259*, 33-45.

[8] M. Ogura, S. Y. Shinomiya, J. Tateno, Y. Nara, E. Kikuchi, M. Matsukata, *Chem. Lett.* **2000**, *29*, 882-883.

[9] S. Abello, A. Bonilla, J. Perez-Ramirez, *Appl. Catal. A Gen.* **2009**, *364*, 191-198.

[10] D. Verboekend, G. Vilé, J. Pérez - Ramírez, *Adv. Funct. Mater.* **2012**, *22*, 916-928.

[11] C. S. Triantafillidis, A. G. Vlessidis, N. P. Evmiridis, *Ind. Eng. Chem. Res.* **2000**, *39*, 907-319.

[12] C. J. Van Oers, W. J. Stevens, E. Bruijn, M. Mertens, O. I. Lebedev, G. Van Tendeloo, P. Cool, *Microporous Mesoporous Mater.* **2009**, *120*, 29-34.

[13] B. Sulikowski, *J. Phys. Chem.* **1993**, *97*, 1420-1425.

[14] R. Gounder, *Catal. Sci. Technol.* **2014**, *4*, 2877-2886.

[15] T. Tago, H. Konno, S. Ikeda, S. Yamazaki, W. Ninomiya, Y. Nakasaka, T. Masuda, *Catal. Today* **2011**, *164*, 158-162.

[16] A. K. Singh, R. Yadav, A. Sakhtivel, *J. Mater. Sci.* **2016**, *51*, 3146-3154.

[17] A. K. Singh, R. Yadav, V. Sudarsan, K. Kishore, S. Upadhyayula, A. Sakhtivel, *RSC Adv.* **2014**, *4*, 8727-8734.

[18] A. K. Singh, R. Yadav, A. Sakhtivel, *Microporous Mesoporous Mater.* **2013**, *181*, 166-174.

[19] J. Ahmadpour, M. Taghizadeh, *C. R. Chimie* **2015**, *18*, 834-347.

[20] M. Bjorgen, F. Joensen, M. S. Holm, U. Olsbye, K. P. Lillerud, S. Svelle, *Appl. Catal. A Gen.* **2008**, *345*, 43-50.

[21] X. Chen, D. Xi, Q. Sun, N. Wang, Z. Dai, D. Fan, V. Valtchev, J. Yu, *Microporous Mesoporous Mater.* **2016**, *234*, 401-408.

[22] A. Carrero, G. Vicente, R. Rodriguez, M. Linares, G. L. Del Peso, *Catal. Today* **2011**, *167*, 148–153.

[23] T. Tago, H. Konno, S. Ikeda, S. Yamazaki, W. Ninomiya, Y. Nakasaka, T. Masuda, *Catal. Today* **2011**, *164*, 158–162.

[24] M. Zhang, L. Wang, Y. Chen, Q. Zhang, C. Liang, *J. Energy Chem.* **2016**, *25*, 539-544.

[25] S. Gopalakrishnan, A. Zampieri, W. Schwieger, *J.* Catal. **2008**, *260*, 193–197.

[26] J. Xing, L. Song, C. Zhang, M. Zhou, L. Yue, X. Li, *Catal. Today* **2015**, *258*, 90-95.

[27] D. Verboekend, M. Milina, J. Perez-Ramirez, *Chem. Mater.* **2014**, *26*, 4552-4556.

[28] Y. Y. Wang, T. H. Dang, B. H. Chen, D. J. Lee, *Ind. Eng. Chem. Res.* **2012**, *51*, 9959-9965.

[29] Y. Y. Wang, H. H. Wang, T. L. Chuang, B. H. Chen, D. J. Lee, *Energy Procedia* **2014**, *61*, 933-936.

[30] S. Semwal, A. K. Arora, R. P. Badoni, D. K. Tuli, *Bioresour. Technol.* **2011**, *102*, 2151-2161.

[31] A. Srivastava, R. Prasad, *Renew. Sustain. Energy Rev.* **2000**, *4*, 111-133.

[32] A. P. S. Chouhan, A. K. Sharma, *Renew. Sustain. Energy Rev.* **2011**, *15*, 4378-4399.

[33] D. E. Lopez, J. G. Goodwin Jr, D. A. Bruce, E. Lotero, *Appl. Catal. A Gen.* **2005**, *295*, 97-105.

[34] Y. Essamlali, O. Amadine, A. Fihri, M. Zahouily, *Renewable Energy* **2019**, *133*, 1295-1307.

[35] L. Du, S. Ding, Z. Li, E. Lv, J. Lu, J. Ding, *Energy convers. Manage.* **2018**, *173*, 728-734.

[36] M. Bandyopadhyay, N. Tsunoji, R. Bandyopadhyay, T. Sano, *Reac. Kinet. Mech. Cat.* **2019**, *126*, 167-179.

[37] M. Bandyopadhyay, N. Tsunoji, T. Sano, *Catal. letters* **2017**, *147*, 1040-1050.

[38] L. J. Konwar, P. Mäki-Arvela, P. Begum, N. Kumar, A. J. Thakur, J. P.Mikkola, R. C. Deka, D. Deka, *J Catal.* **2015**, *329*, 237-247.

[39] M. Pramanik, A. Bhaumik, *Chem. Eur. J.* **2013**, *19*, 8507-8514.

[40] M. Sasidharan, A. Bhaumik, *J Sol-Gel Sci. Technol.* **2012**, *61*, 367-373.

[41] M. Bandyopadhyay, R. Bandyopadhyay, S. Tawada. Y. Kubota, Y. Sugi, *Appl. Catal. A Gen.* **2002**, *225*, 51-62.

[42] R. Thakkar, R. Bandyopadhyay, *J Chem Sci.* **2017**, *129*, 1671-1676.

[43] R. Gomes, A. Bhaumik, *J. Solid State Chem.* **2015**, *222*, 7-11.